Ethiopian Journal of Science and Sustainable Development

e-ISSN 2663-3205 *Volume 7 (1), 2020*

Journal Home Page: www.ejssd.astu.edu.et

Research Paper

Investigation of Laser Surface Treatment on the Microstructure and Mechanical Properties of AlSiMn Alloy

Moera Gutu Jiru* and Habtamu Beri

Department of Mechanical Design and Manufacturing Engineering, Adama Science and Technology, P. O. Box 1888, Adama, Ethiopia

Article Info

Keywords:
Mechanical property
Laser remelting
Aluminum
Silicon

Abstract

This work investigates high-temperature properties of AlSiMn alloy after laser remelting by continuous mode CO_2 laser energy. Substrate materials were prepared after solutionized heat-treated at 510ºC for 5 h followed by artificially aged at 160ºC for six hours. The result of the finding showed high improvement in mechanical properties by 80% of heat-treated samples. The formation of fine dendrite microstructure, rode like larger secondary dendrite and sound metallurgical bonded morphology played a great role. The maximum laser modified thickness of 2.23 mm was achieved.

1. Introduction

The durability of engineering materials depends on both surface and bulk material properties, but most significantly, on surface properties. A good surface property enhances durability of the component by protecting the bulk material from external damages caused due to environments such as corrosion and any mechanical effects such as wear. Al-Si-Cu-Mg alloys are widely used to manufacture cylinder blocks and covers of the engine for small passenger cars because of their good strength at high temperature. Long back et al. (1979) observed that the wear resistance of Al-Si alloys increases with increasing silicon content until the eutectic composition, i.e. 12 wt%. Hwang et al. (2009) observed that addition of 0.45 wt% Mg to type 319 aluminum alloy (Al-6.7Si-3.75Cu) increased the strength of the alloy, although at the expense of ductility. The addition of manganese further improves the high-temperature strength of the aluminum alloys. Manganese addition in Al-7Si-3.8Cu-0.5Fe alloys is usually used to neutralize the detrimental effects of β-Al_5FeSi by transforming it to the α-Al_{13} (Mn, Fe)$_4$ Si_2 phase (Hwang et al., 2008). Liao et al. (2017) developed high manganese aluminum alloy, Al-12Si-4Cu-1.2Mn by casting route. It displayed high ultimate tensile strength (more than 132 MPa) at 250°C.

Apart from the high tensile strength for cylinder blocks, high surface hardness and good tribological behavior are also needed. Laser surface melting (LSM) can be a potential process for improving the surface characteristics. LSM has been applied for improving the hardness of cast alloys as well as fabricating the product from the powder. In this process, cooling rates of the order of 10^5 to 10^8 K/s are obtained that helps in achieving the refined microstructure (Sahoo et al., 2015). Pinto et al. (2003) carried out LSM of Al-15Cu alloy and observed about three times increase in the hardness. Abbas et al. (2006) carried out LSM of magnesium alloys, AZ31 and AZ61, using a 1.5 kW high power diode laser (HPDL). A significant improvement in the hardness and wear resistance was

*Corresponding author, e-mail: jirata2010moti@gmail.com

https://doi.org/10.20372/ejssdastu:v7.i1.2020.134

observed with a grain size of about 5 μm. Zhang et al. (2008) enhanced the tribological properties of AM50 magnesium alloy by LSM with a 2 kW continuous wave CO_2 laser. A significant improvement in microhardness and wear resistance was observed, although there was no significant effect on the coefficient of friction. Cabeza et al. (2012) used LSM to repair the surface of a maraging steel, 14 Ni (200 grade), in different heat treatment conditions using high power solid Nd-YAG laser.

The effect of LSM on corrosion behavior has also been studied. Conde et al. (2000) carried out LSM of austenitic, ferritic and martensitic stainless and observed an increase in the corrosion resistance provided the correct processing parameters were used. Majumdar et al. (2003) observed that LSM of a commercial Mg alloy, MEZ (Zn 0.5%, Mn 0.1%, Zr 0.1%, rare earth elements 2%, Mg remaining percentage), resulted in an increase of its hardness, wear-resistance and corrosion resistance. Osorio et al. (2008) investigated the effect of LSM on the corrosion resistance of Al-9Si casting alloys. As-cast samples were remelted using a continuous 1 kW CO_2 laser. However, the corrosion resistance got reduced due to LSM.

Kang et al. (2016) carried out selective laser melting of mixtures of Al-12 Si alloy and Si powders to improve the wear performance. The final composition achieved was Al-18Si. Aboulkhair et al. (2016) improved the fatigue performance of selective laser melted Al-Si10Mg alloy. Laorden et al. (2017) reported selective laser surface melting of A356 and aluminum matrix composite reinforced with SiC particles (A356/10% SiC particles). Several researchers investigated the polishing of the surface using laser irradiation. Ukar et al. (2010) reported 90% surface roughness reduction after laser polishing of DIN 1.2379 tool steel using CO_2 and high power diode laser. The mean roughness value obtained was below 0.5 μm. Pfefferkorn et al. (2014) reported the advantages of pulsed laser polishing of S7 tool steel. They observed that a larger melt pool diameter provided a smoother surface than the smaller one. (Pfefferkorn, 2017) have presented interesting results on pulsed laser micro-structuring of the surface of Ti-6Al-4V alloy.

This research is mainly focused to fill the gap that found from the research of Hwang et al. (2008) and Liao et al. (2017), in which laser surface treatment was not conducted. Therefore, this work mainly focused on the investigation of laser surface treatment and studied the effect of laser power, scanning speed on micro-hardness and morphology of the modified surface. The main objective of this work is therefore to improve mechanical properties such as hardness and scratch resistance, and investigation of the effect of laser beam energy density on the depth of modified surface and micro hardness of laser modified surface.

2. Materials and Methods

For this experiment work, samples were prepared in the dimensions of $160 * 55 * 10$ mm^3 using aluminum from the cast AlSiMn block. Chemical composition (wt. %) of AlSiMn substrate before laser remelting is given in Table 1. Laser remelting was conducted along the width direction (55 mm), single bead without overlapping and multiples of beads formed on the same sample up to six beads processed by different laser parameters from 1.7 kW to 2.2 kW laser power, and from 300 mm/min to 550 mm/min laser scanning speed. The overall laser parameters used for the experiment are given in Table 2. Laser energy density was calculated from laser power, scanning speed and laser beam diameter.

Table 1: Chemical composition (wt.%) of AlSiMn substrate before laser remelting

	Si	**C**	**Fe**	**Mn**	**Mg**	**Cu**	**Al**
Wt.%	11.03-12.01	0.21	1.02	2.5-3.5	0.2	0.13	84.91

After laser melting was completed, the metallographic study was conducted by cutting some portion of the laser-remelted region and polished in cross-section direction in order to observe both the remelted and substrate portion and to reveal the thickness of laser remelted region. After polishing with different Silicon carbide emery sheets starting from 250, 600, 1200 and 2000 grades and final mirror, polishing was made by smooth cloth with the help of chemical Sillvo. The mirror-polished samples were etched at room temperature using standard chemical solutions prepared from 1mL HF, 1.5 mL HCl and 2.5 mL HNO_3 in the solution of 95 mL purified water. The etching was made by rubbing the samples by applying chemicals on the mirror-polished surface using clean cotton, for 6–8 S, then washing with water to neutralize to avoid further

etching. The dried samples were observed by optical microscopy to investigate microstructure and grain size. The morphology of laser-remelted region was studied using the help of high-resolution electron microscopy called Field Emission Scanning Electron Microscopy (FESEM). In order to study the chemical composition after laser remelting both elemental mapping and weight percentage composition tests were analyzed using Electron Dispersive Spectroscopy (EDS) machine. Different mechanical properties were studied after laser remelting was conducted. The hardnesses of laser-remelted regions were measured by the Vickers hardness testing machine by applying a 3 kg load along the cross-section of the polished surface. Continuous multiple remelting beads without overlapping were carefully maintained on one side of the sample of 5 mm plate prepared from the 10 mm blocks. The tensile specimens were prepared by cutting a portion of laser-treated area by cutting using wire EDM machine. The results of all the experiments were discussed in the result and discussion section. Table 1 shows the chemical composition of the substrate material. Laser energy density was calculated as follows (Jain et al., 1981):

$$E = \frac{P}{vd},$$

Where, P is laser power, v is scan speed and d is laser beam diameter.

Table 2: Laser process parameters of laser remelting

Laser beam energy density (J/mm^2)	Laser power (kW)	Laser scanning speed (mm/min)	Laser beam diameter (mm)
44.53	2.2	550	5.39
46.76	2.1	500	5.39
49.47	2.0	450	5.39
52.93	1.9	400	5.39
57.28	1.8	350	5.39
63.08	1.7	300	5.39

3. Result and Discussion

In this section, the results of the all experiments were discussed in detail. The remelted layer thickness, microstructure, grain size, surface morphology and elemental mapping as well as tensile properties were investigated.

3.1. The remelted thickness

Figure 1 shows the cross-sectional view of laser-remelted samples measured by digital microscopy. The top half-moon shape represents the remelted thickness and width in cross-section view. The remelting quality is sufficiently made without defects like cracks or unmelted conditions. The depth and width of a laser remelted layer thicknesses are presented in Figure 2 (a, b). The effect of heat treatment on the geometry of laser-remelted thickness was investigated. For samples processed with the same laser parameters, both the depth and width of remelted layers are more for unheated samples and less for solutionized heat-treated and artificially aged samples. As a laser energy density was increased from 44.53 J/mm^2 to 63.08 J/mm^2, the remelted depth was linearly increased for both samples. For heat-treated samples, the minimum depth was 1.14 mm and while the maximum depth was 1.77 mm. When laser energy density was maximum at 63.08 J/mm^2. The remelted depth of untreated samples was nearly closed with heat-treated samples up to the energy density of 52.93 J/mm^2 while after which it was increased and a maximum of 2.29 mm at high laser energy used. Since heat treatment has improved the hardness of the material, after laser remelting less remelting thickness was measured than, unheated samples.

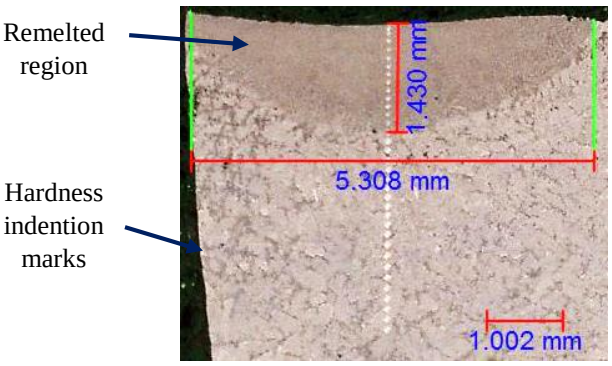

Figure 1: Cross-section view of laser remelted samples processed by different laser energies, (X20); heat-treated sample 44.53 J/mm^2

The response of heat-treated samples even at high laser energy was not very sensitive. The width of a laser remelted layers were 5.31 mm to 5.86 mm at low and high laser energies for heat-treated samples. While for untreated samples, the remelted layer was from 4.87 mm to 6.34 mm. Heat treatment prior to laser treatment has improved the hardness of the material. The thickness of

the laser-remelted surface plays a significant role to protect the surface from any damages such as wear and corrosion. In this regard, the more remelted layer thickness formed has more advantageous than less remelted layers thickness formed. To maintain sufficient thickness of laser modified surface requires a careful understanding of process parameters and applications of the material in which it works. In other laser surface modifications like alloying, this may be more costly due to the cost of alloying elements added to the base material. The variation of laser modified surface thickness was due to laser process parameters and heat treatment conditions. Wong et al. (1997) reported laser remelting of aluminum alloy and indicated that remelted depth and width were increased with an increased in laser power density.

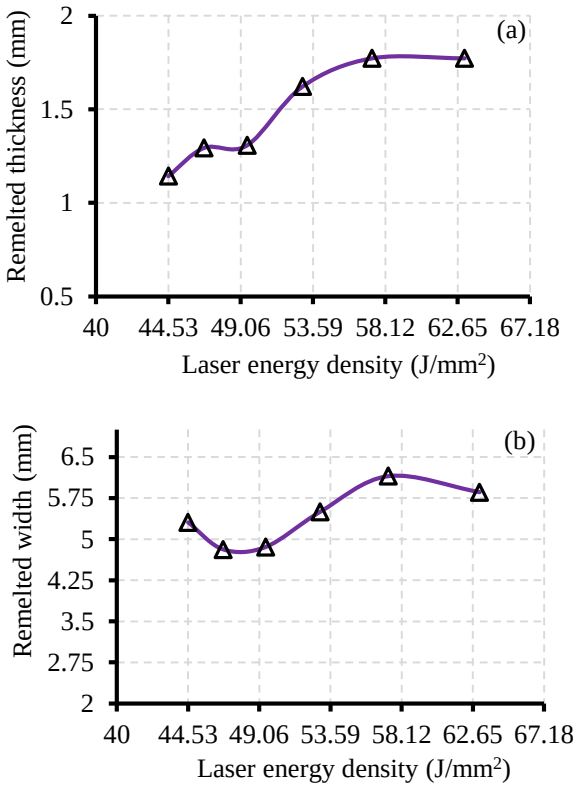

Figure 2: The effect of laser energy density on laser remelted thicknesses (a) and remelted width (b).

3.2. Microstructure and grain size

The properties of a material depend on the type of material and manufacturing technique used to produce the part. For metals and its alloys, the orientation and gain structure formed in the microstructure play a critical role. All improvements to make high-performance alloys have been under way for many decades. A laser surface modification like remelting the existing material is one method under attention. The microstructures of heat-treated and untreated samples after laser remelting in the same laser process parameters were compared. Figure 3a shows the microstructure of laser heat-treated samples and Figure 3b is microstructure before laser remelting. The grain structures are small and major alloying element silicon was revealed in the morphology as silicon rods and silicon plates (Figure 3b). The smaller grain size formed was due to the heat treatment effect. Since heat treatment by itself improves material properties by making a rearrangement of grain structure during heating followed by aging or cooling process. In this case, after solutionized heat treatment in an electrical furnace at 510°C for 5 h and artificial aging at a controlled temperature of 160°C for 6 h. This is an improvement in microstructure by alloying homogenous grain structure than unheated treated samples.

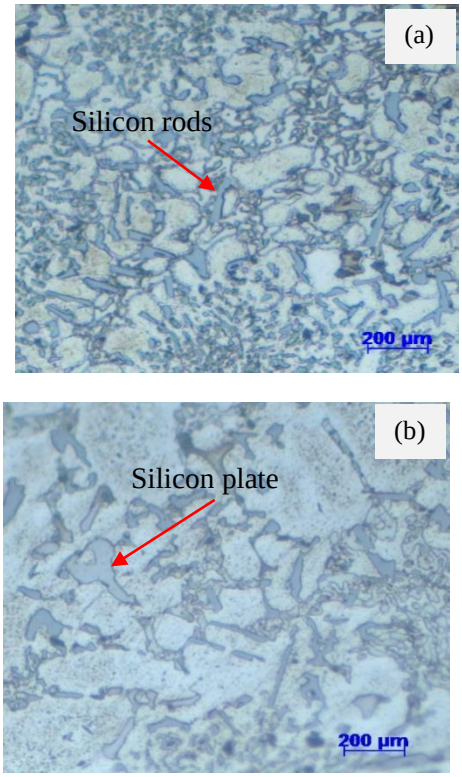

Figure 3: Microstructure (a) after laser remelting and (b) before laser remelting

Figure 4(a-f) shows the microstructure of heat-treated samples after laser remelting. The microstructure formed was different when different laser energy densities were used. The dendrite microstructures were formed in different places for the same material processed by the same laser energy density. The dendrite grains formed from the interface and grow in the direction of the melt pool center along with the direction of solidification. Figure 4(e, f) shows the direction of dendrite grows in the arrows head indicated. During laser remelting, the substrate portion absorbs more heat and dissipated along with its parts, so that it acts as a cooling initiator. The solidification starts from the interface and proceeds up the surface. The grain structure was very closely arranged and networks of small dendrite cells were formed when laser energy densities of 44.53 J/mm^2, 46.76 J/mm^2, and 49.47 J/mm^2, as shown in Figures 4(a, b, c). The dendrite structures were more lateral growth when the laser energy was started increasing from 52.93 to 63.08 J/mm^2 as illustrated in Figures 4(d, e, f). The high energy caused more remelted layer thickness deeper, so that the cooling rate was slower than, other samples processed by low laser energies. Because of this effect, the dendrite arm structures got sufficient time to grow. This was visible in a typical microstructure shown in Figure 4(f).

During laser remelting and solidification processes, primary α-Al and Al-Si eutectic structures of fine-grain structures were formed. Because of a rapid solidification process, fine dendrite grains are formed near the top and at the center of remelted layers. The interface grain structure mostly contains secondary dendrite formations while HAZ has columnar grains. The dendrite arm spacing and grain sizes are dependent on cooling and solidification rates. Rapid cooling enhanced fine microstructures of small grain sizes, small dendrite cells, which was visible in Figure 4(f). The solidification starts from an interface and higher solidification rate achieved near the center and top portion. The top and center remelted regions have small grain sizes, small dendrite cells, and dendrite arm spacing than interface-remelted layers.

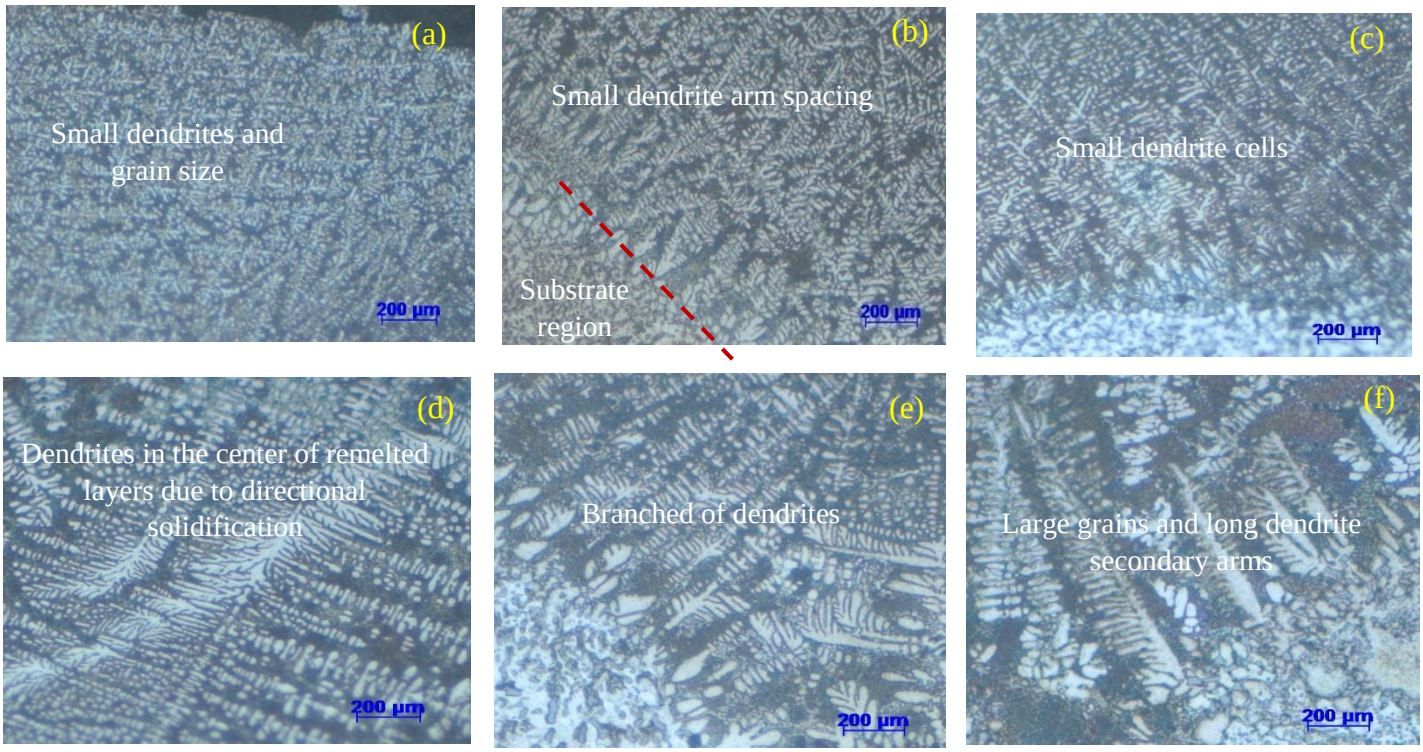

Figure 4: Microstructure of heat-treated samples after laser remelting at different laser energies (X40); (a) 44.53 J/mm^2, (b) 46.76 J/mm^2, (c) 49.47 J/mm^2, (d) 52.93 J/mm^2, (e) 57.28 J/mm^2 and (f) 63.08 J/mm^2.

The microstructure of heat affected zone was different from the laser remelted region. The columnar grain structures are formed due to heating effects without remelting. Figure 5(a-b) shows a typical microstructure of heat affected zones for both heat-treated and untreated samples after laser remelting. The grain sizes are bigger and different from laser remelted regions. There is no melting takes place, but due to heating effect, the grains are reallocated and formed large grains of secondary dendrites. The dendrite arm spacing was bigger in untreated samples than heat-treated samples.

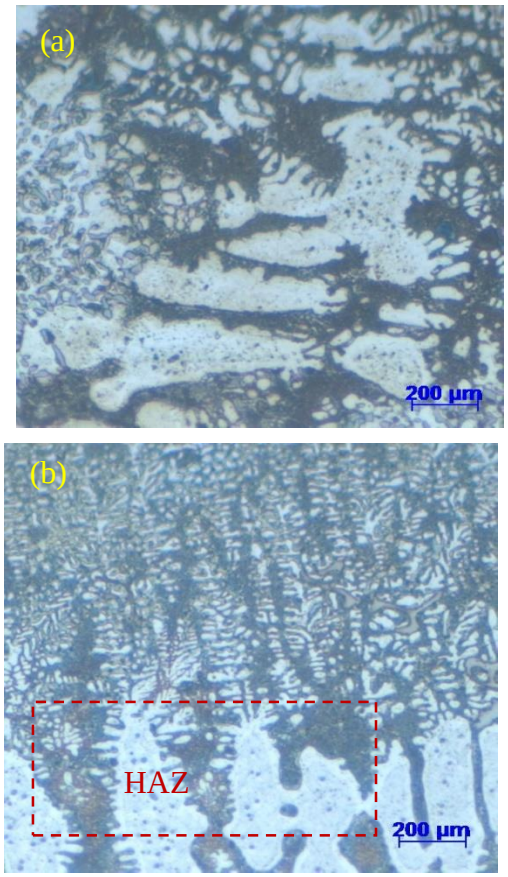

Figure 5: Microstructure of (a) heat affected zone after laser remelting and (b) interface zone of laser re-melted heat affected zone (HAZ).

Figure 6 illustrates the average grain size of the laser-remelted samples with respect to laser process parameters. The grain size of both heat-treated and untreated samples was compared which are processed by the same laser parameters. The results show the average grain sizes of unheated treated samples were bigger than heat-treated samples. At the minimum laser energy density of 44.53 J/mm^2, average grain size was 26.45 µm and 30.23 µm, for heat-treated and untreated samples, respectively. For both samples, the maximum grain size was 29.78µm and 42.69 µm, formed at the maximum laser energy density of 63.08 J/mm^2. This may be due to more energy created larger remelted layer thicknesses, and deeper remelted thickness so that cooling time is more. The cooling time of deeper remelted thickness was more than the cooling time of thin remelted thickness. A short cooling time or high cooling rate allows the formation fine microstructure of samples processed by less laser energy than theses processed by higher laser energies. The grain size of the heat-treated sample before laser remelting was 64.76 µm, while it was larger as 74.18 µm, for untreated samples.

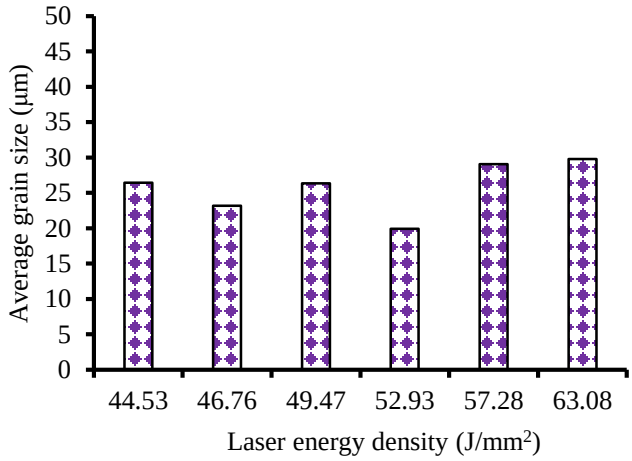

Figure 6: The effect of laser energy density on average grain diameter after laser remelting

The larger grain sizes were formed in the heat-affected regions of both materials. The average grain size in HAZ for the heat-treated sample was 74.68 µm, while for untreated samples 81.42 µm. The grain sizes are visible as observed in the microstructure images. The formation of networks of small dendrite cells in the microstructure was clustered near the top remelted layers. The small grain sizes are formed at the center of the remelted layer while columnar grains are revealed near the interface region as bigger grain sizes. The fine microstructure will boost mechanical properties of the material like its microhardness and wear performances.

3.3. Surface Morphology and Chemical Composition

The quality of laser-remelted samples was investigated from surface morphology conducted by FESEM at higher magnifications. The presence of defects in the material affects performance and durability of the material and should be avoided. In order to evaluate the quality of laser remelted layer thickness of both heat-treated and untreated samples, a morphology study was conducted like the one given in Figure 7(a, b) for heat-treated samples. The result confirms the sound metallurgical bonding formed during laser remelting. The connection of each grain with neighboring grains formed without forming defects like porosity and cracks. Figure 8 shows elemental mapping after laser remelting. It confirms that silicon decomposition is about 13%.

3.4. Investigation of mechanical properties

The hardness in cross-section of remelted thickness was conducted and the effect of laser process parameters was investigated. The surface scratch test for evaluating deformation resistance of laser remelted samples was also discussed in this subsection.

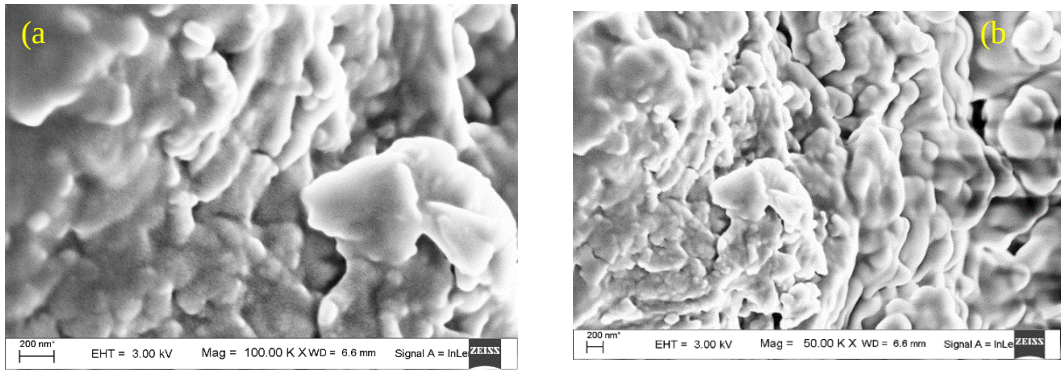

Figure 7: The Morphology of heat-treated sample after laser remelting at different magnifications (a) 100 k.and (b) 50 k

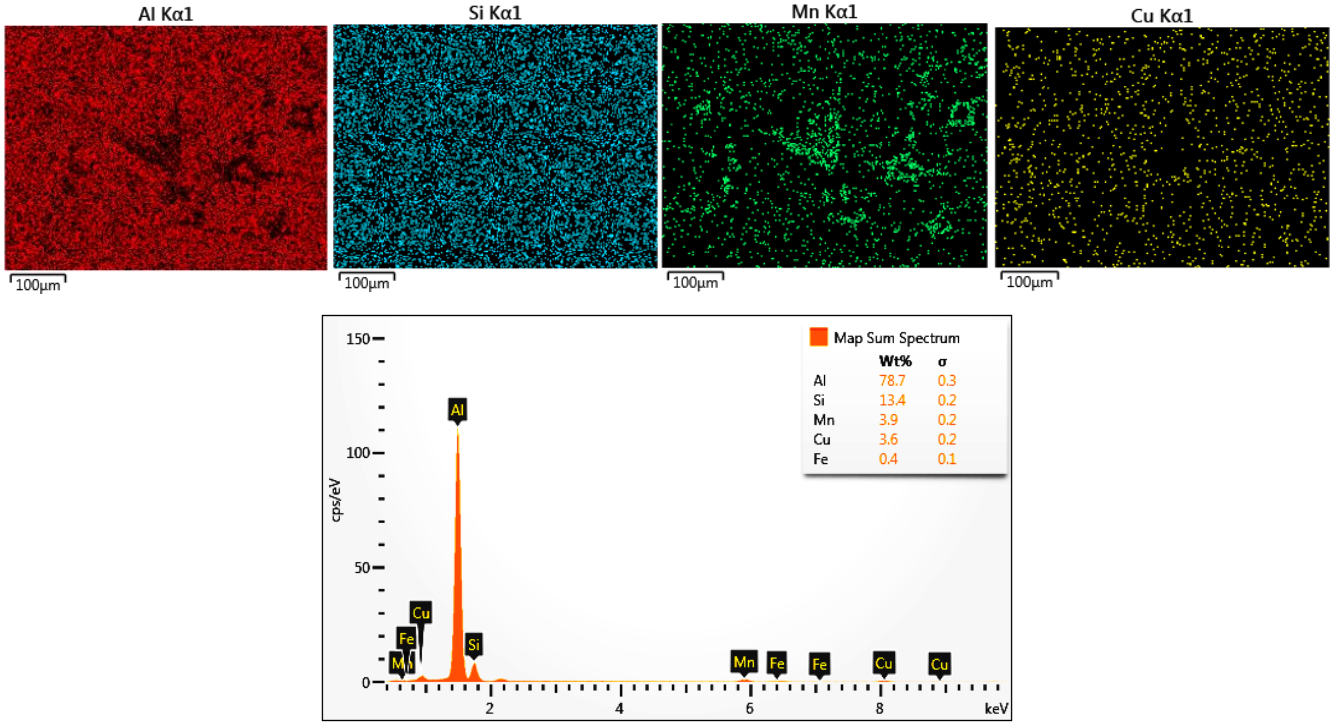

Figure 8: Solutionized heat-treated sample after laser surface remelting of sample processed by 1.9 kW laser power. morphology of remelted region and composition

3.4.1 Microhardness

The hardness of the laser-remelted layer was measured in cross-section from the top of the laser-remelted region to the substrate region (Figure 1). The hardness of the laser-remelted region is much more improved than the substrate material. However, the hardness is not uniform throughout the remelted layer, which is because of the grain structure and orientation is different from the remelted layer. Figure 9(a-d) shows the microhardness values of laser-remelted samples for both heat-treated and untreated samples in comparison. In order to observe the effect of laser energy density on the microhardness, six samples were processed by different laser parameters for heat-treated and untreated samples. The hardness of AlSi material prior to laser remelting has an average hardness of 81.67 $HV_{0.3}$ and 78.86 $HV_{0.3}$, for solutionized heat-treated and untreated samples.

The maximum microhardness of 175.35 $HV_{0.3}$ for heat-treated samples near the top remelted region while untreated sample microhardness was 186.75 $HV_{0.3}$. For the first two laser energy densities, the hardness of untreated samples was greater than heat-treated samples. However, when laser energy density was increased, the hardness of heat-treated samples is higher than in untreated samples. Because of the heat applied is sufficient to make a hardening effect of heat-treated samples. For heat-treated samples after laser remelting, the maximum hardness of 203.59 $HV_{0.3}$ was measured for samples processed by 49.47 J/mm^2 laser energy densities. For a heat-treated sample, the maximum microhardness of 205.95 $HV_{0.3}$ was achieved for a sample processed by 46.76 J/mm^2. The effect of increasing laser energy density has a reduced hardness of both heat-treated and untreated samples. The minimum hardness was measured for samples processed by the maximum energy density of 63.08 J/mm^2. This is because of the more energy used, caused deeper remelted thickness of the material, where the grain sizes were coarse. This was confirmed from the result of the average grain diameter discussed in the previous section. The hardness was more, nearly a little far from the top laser remelted layer thickness since the top portion was mainly aluminum. The hardness also randomly decreasing in laser remelted layer thickness towards the substrate material. Heat-affected zone also shows improved hardness than the substrate material.

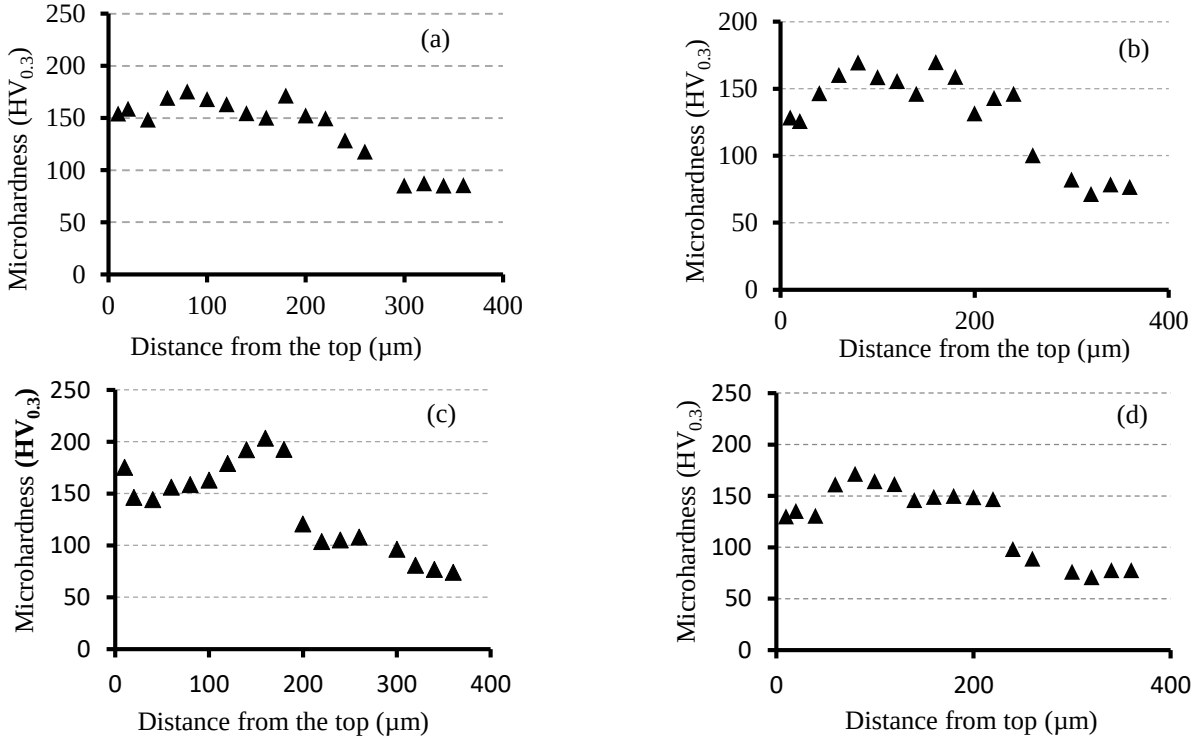

Figure 9: Microhardness of laser remelted samples at different laser energy densities; (a) 44.53 J/mm^2, (b) 46.76 J/mm^2, (c) 49.47 J/mm^2 and (d) 52.93 J/mm^2

4. Conclusion

In this piece of work, the laser surface melting of Al-12Si-4Cu-1.2Mn alloy was successfully achieved. The dendrite microstructure and refined grain size provided, improved mechanical properties after laser surface melting. There was about a 2.5 times increase in the microhardness of heat-treated samples after LSM. Heat treated samples also showed improved in mechanical properties. Hardness was more, nearly a little far from the top laser remelted layer thickness since the top portion was mainly aluminum. The hardness also randomly decreasing in laser remelted layer thickness towards the substrate material. Heat-affected zone also shows improved hardness than the substrate material. Laser remelting has refined average grain size and improved microhardness.

Reference

Abbas, G., Li, L., Ghazanfar, U. and Liu, Z. (2006). Effect of high power diode laser surface melting on wear resistance of magnesium alloys, *Wear*, 260(1): 175–180.

Aboulkhair, N.T., Maskery, I., Tuck, C., Ashcroft, I. and Everitt, N.M. (2016). Improving the fatigue behavior of a selectively laser melted aluminium alloy: *Influence of heat treatment and surface quality, Materials and Design*, 104: 174–182.

Campbell, F.C. (2012). Phase Diagram Applications. Phase Diagrams: Understanding the Basics, Materials Park, Ohio: ASM International, pp. 290―291.

Clarke, J. and Sarkar, A.D. (1979). Wear characteristics of as-cast binary aluminium-silicon alloys, *Wear*, 54(1): 7–16.

Conde, A., Colaço, R., Vilar, R. and de Damborenea, J. (2000). Corrosion behavior of steels after laser surface melting, *Materials and Design*, 21(5): 441–445.

Hwang, J.Y., Doty, H.W. and Kaufman, M.J. (2008). The effects of Mn additions on the microstructure and mechanical properties of Al–Si–Cu casting alloys, *Materials Science and Engineering: A*, 488(1): 496–504.

Hwang, J.Y., Banerjee, R., Doty, H.W. and Kaufman, M.J. (2009). The effect of Mg on the structure and properties of Type 319 aluminum casting alloys, *Acta Materialia*, 57(4): 1308–1317.

Jain, A.K., Kulkarni, V.N. and Sood, D.K., (1981). Pulsed laser heating calculations incorporating vaporization, *Applied physics*, 25(2):127―133.

Kang, N., Coddet, P., Liao, H., Baur, T. and Coddet, C. (2016). Wear behavior and microstructure of hypereutectic Al-Si alloys prepared by selective laser melting, *Applied Surface Science*, 378: 142–149.

Liao, H., Tang, Y., Suo, X., Li, G., Hu, Y., Dixit, U.S. and Petrov, P. (2017). Dispersoid particles precipitated during the solutionizing course of Al-12 wt% Si-4 wt% Cu-1.2 wt% Mn alloy and their influence on high temperature strength, *Materials Science and Engineering: A*, 699: 201―209.

Laorden, L.M., Rodrigo, P., Torres, B. and Rams, J. (2017). Modification of microstructure and superficial properties of A356 and A356/10% SiC by Selective Laser Surface Melting (SLSM), *Surface and Coatings Technology*, 309: 1001–1009.

Majumdar, J.D. and Manna, I. (2003). Laser processing of materials, *Sadhana*, 28(3-4): 495–562.

Pfefferkorn, F.E., Duffie, N.A., Morrow, J.D. and Wang, Q. (2014). Effect of beam diameter on pulsed laser polishing of S7 tool steel, *CIRP Annals*, 63(1): 237–240.

Pinto, M.A., Cheung, N., Ierardi, M.C.F. and Garcia, A. (2003). Microstructural and hardness investigation of an aluminum–copper alloy processed by laser surface melting, *Materials Characterization*, 50(2): 249–253.

Osório, W.R., Cheung, N., Spinelli, J.E., Cruz, K.S. and Garcia, A. (2008). Microstructural modification by laser surface remelting and its effect on the corrosion resistance of an Al–9wt% Si casting alloy, *Applied Surface Science*, 254(9): 2763–2770.

Sahoo, C.K., Sahu, J.K. and Masanta, M. (2015). Effect of pulsed Nd: YAG laser parameters in preplaced TiC coating on aluminium substrate, in Lasers Based Manufacturing: *5th International and 26th All India Manufacturing Technology, Design and Research Conference*, Springer, New Delhi.

Ukar, E., Lamikiz, A., López de Lacalle, L.N., Del Pozo, D. and Arana, J.L. (2010). Laser polishing of tool steel with CO2 laser and high-power diode laser, *International Journal of Machine Tools and Manufacture*, 50(1): 115–125.

Wong, T.T., Liang, G.Y. and Tang, C.Y. (1997). The surface character and substructure of aluminium alloys by laser-melting treatment, *Journal of Materials Processing Technology*, 66(1): 172–178.

Zhang, Y., Chen, J., Lei, W. and Xv, R. (2008). Effect of laser surface melting on friction and wear behavior of AM50 magnesium alloy, *Surface and Coatings Technology*, 202(14): 3175–3179.